INTERCOMPARISON OF WAVE DATA HINDCAST ON LAKE ERIE

Masataka Yamaguchi, Yoshio Hatada and Hirokazu Nonaka

Department of Civil and Environmental Engineering, Ehime University
Matsuyama, Ehime Prefecture, Japan

1. INTRODUCTION

Modern wave prediction models have been classified into three categories, depending on how the wave-wave interaction term which plays a dominant role in the wave growth, is incorporated into the model. Yamaguchi et al. (1984, 1987) developed several wave prediction models belonging to the first and second generations and has verified their applicability, based on comparisons with measurement wave data on bodies of water with a variety of horizontal scales, such as ; Lake Kasumigaura (5 - 10 km), Lake Biwa (15 - 30 km), the Seto Inland Sea (50 - 100 km), the Japan Sea (500 - 1000 km) and the Pacific Ocean (more than 1000 km). Among them, a backward ray tracing model(BRTM) for shallow water waves is a decoupled propagation model, belonging to the first generation model, which does not take into account the wave-wave interaction term in the source term and estimates energy dissipation associated with wave breaking by a saturated spectrum. In spite of that, detailed comparisons with measurement data have verified that the model makes it possible to properly estimate waves with high computational efficiency, making use of a nested grid system with fine space resolution.

In recent years, the third generation wave models, particularly WAM(The WAMDI group, 1988; Günther et al., 1992) and SWAN(Booij et al., 1999), which make it possible to reproduce the wave growth characteristics without imposing any restriction on the spectrum, by directly performing an approximate computation for the wave-wave interaction term, have been developed and are now open to the public domain. Their verification tests, based on comparisons with measurement wave data, have been conducted on a worldwide scale, including Japan. As an example, Lalbeharry et al. (2001) reported their verification test results on Lake Erie of the Great Lakes.

In this study, wave hindcasting at each of 3 buoy stations on Lake Erie using BRTM is made under the same bathymetry and wind input conditions as Lalbeharry et al. (2001), which were kindly provided by Roop Lalbeharry of the Meteorological Service of Canada, Environment Canada. Intercomparison is made among BRTM-based wave data, WAM-based wave height data given by Roop Lalbeharry and measurement wave data.

2. CHARACTERISTICS OF MEASURED WIND AND WAVE DATA ON LAKE ERIE

Lake Erie has a laterally-prolonged scale of about 400 km in the west-east direction and about 100 km in the north-south direction, which for references of scales, would situate it between the Seto Inland Sea with a directional fetch of 50 to 100 km and the Japan Sea with a directional fetch of 500 to 1000 km. Figure 1 illustrates a grid of 0.05 degrees distance set on the lake by Lalbeharry et al.(2001), contourlines of water depth and location of 3 buoys deployed for wind and wave measurement. Shallow water area widely extends in Lake Erie and the deepest water depth is only 58 m around the position in lat. 42° North and in long. 80° West. Lake Erie is almost surrounded by flat land that is substantially regarded as a closed basin. The ID numbers of the buoys with their water depth and nationalities are ; 45005 (14.6 m, USA), 45132 (22.0 m, Canada) and 45142 (27.0 m, Canada), respectively. The height of the anemometer equipped to each buoy is 5 m over the lake. Figure 2 shows a distribution of directional fetch at each buoy. The directional fetch at either B45005 or B45142 ranges from 20 km to 300 km due to a laterally-prolonged lake area, but the direction width of a fetch exceeding 100 km is at most 45 degrees and rather narrow. On the other hand, B45132 located at the north side in middle

area of the lake, has a relatively broad direction width from WSW to E with a fetch from 80 km to 160km.

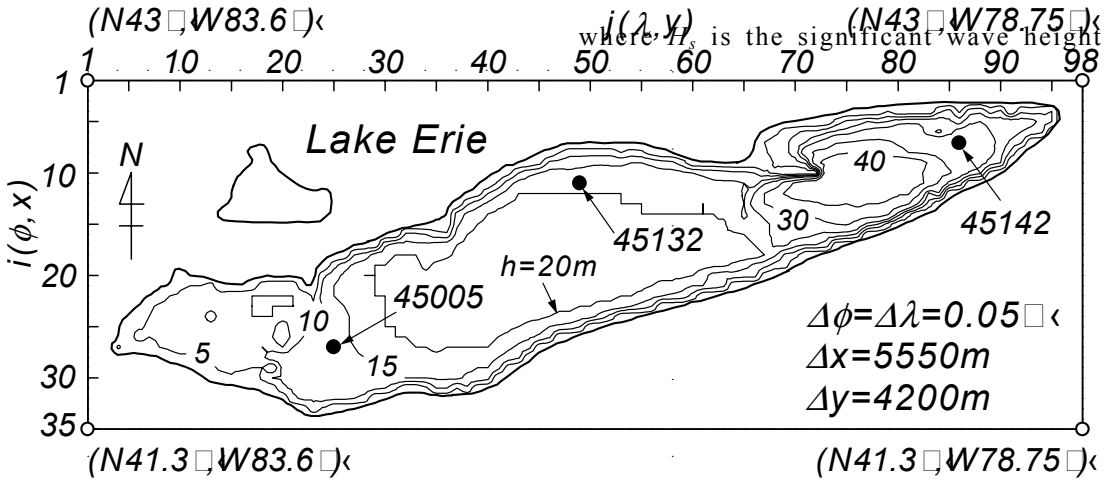

Figure 1. Grid on Lake Erie, contourline of water depth and location of each buoy.

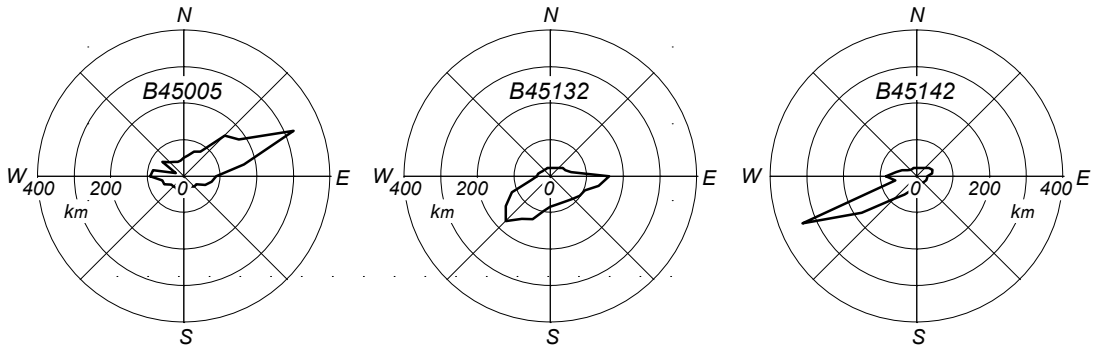

Figure 2. Distribution of directional fetch at each buoy.

Measurement data of winds and waves were extracted from " http://www.ndbc.noaa. gov/ " by the National Data Buoy Center for B45005, and from "http://www.meds-sdmm. dfo-mpo.gc.ca/meds/ Databases/WAVE/WAVE_e.htm" for B45132 and B45142. The data represent hourly wind speed and direction, wave height and wave period, over a period of nearly one month, from October 22 to November 22, 2000. Significant wave period is calculated by multiplying mean wave period at B45142 by 1.2 or multiplying peak period at either B45132 or B45142 by 0.91.

Toba(1972) empirically proposed the following 3/2 power law between dimensionless wave height $\tilde{H}_s (= gH_s / u_*^2)$ and dimensionless wave period $\tilde{T}_s (= gT_s / u_*)$

$$\tilde{H}_s = 0.062 \tilde{T}_s^{3/2} \quad (1)$$

where H_s is the significant wave height, T_s the significant wave period, g the acceleration of gravity, u_* the friction velocity defined by $Cd^{1/2}U_{10}$, C_d the drag coefficient and U_{10} the wind speed at 10 m height. For the drag coefficient C_d, an empirical relation by Mitsuyasu and Kusaba(1984) is applied as

$$C_d = \begin{cases} 1.085\text{x}10^{-3} & ; U_{10} \le 8 \text{ m/s} \\ (0.581+0.063U_{10})\text{x}10^{-3} & ; U_{10} > 8 \text{ m/s} \end{cases} \quad (2)$$

Using this relation, 5 m height wind speed data measured at each of 3 buoys is transformed into 10 m height wind speed data.

Figure 3 shows a relation between dimensionless wave height $\widetilde{H}_s$ and wave period $\widetilde{T}_s$ based on hourly measurement data at each buoy, in which a straight line indicates Toba's 3/2 power law. The measurement-based plots at B45005 are in reasonable agreement with the 3/2 power law, but number of individual data deviating from the 3/2 power law, which corresponds to the waves at a decaying stage increases in the order of B45132 followed by B45142. During blowing of the westerly winds, wind waves are predominant at B45005 with a short fetch, while occurrence of swell-like waves may become more frequent at B45132 and B45142 with an increasingly long fetch. A 3/2 power relation is fitted to the measurement data at each buoy using the least square method.

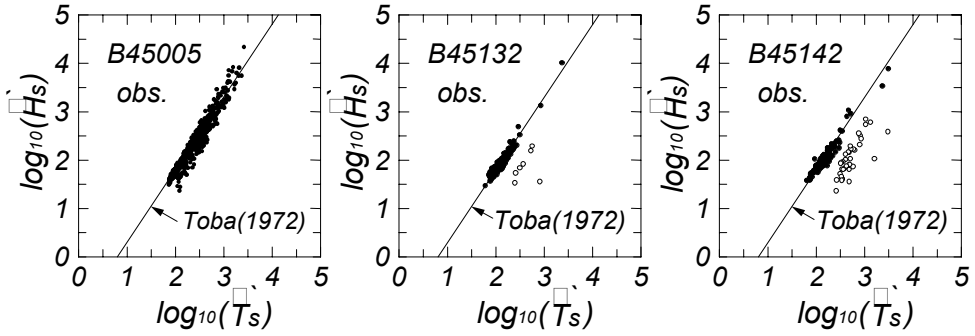

Figure 3. Relation between dimensionless wave height and wave period based on measured data at each buoy.

$$\widetilde{H}_s = a * \widetilde{T}_s^{3/2} \tag{3}$$

The coefficient a is 0.055 at B45005, 0.059 at B45132 and 0.058 at B45142 respectively. The value is nearly constant, ranging from 89 to 95 % to the coefficient of 0.062 by Toba. It may be said that most measurement data used for the verification test consist of wind-generated waves, because individual set of the wave height and period data is approximately satisfied with Toba's 3/2 power law.

3. RESULTS OF VERIFICATION TESTS FOR ESTIMATED WIND AND WAVE DATA

3.1 Conditions for Wave Hindcasting

The wind data provided by Roop Lalbeharry is made by interpolating onto a grid for WAM use with a 0.05 degrees resolution from 3-hourly 10 m height wind data with a 24 km resolution, initially obtained by CMC (Canadian Meteorological Centre). The period is about one month, from October 22 to November 22, 2000. As well, the WAMS (for shallow water)-based and WAMD (for deep water)-based wave data provided by Roop Lalbeharry are 3-hourly wave height data at each of 3 buoys over the same period as the wind data. This comparative study makes use of the WAMS (WAM)-based wave height data which gives a better agreement with the measured data.

A spherical grid for WAM use with a 0.05 degrees resolution is transformed into a rectangular grid for BRTM use with a 5550 m resolution in the north-south direction (x-axis) and a 4200 m resolution in the west-east direction (y-axis), because BRTM is formulated on a Cartesian coordinate system. The number of frequency data used is 28, ranging from 0.073 to 0.959 Hz which is successively obtained from f_{i+1}/f_i=1.1 and f_1=0.05 Hz, and the number of direction data is 37 equally divided with an increment of 10 degrees on the whole circle. The condition of zero directional spectrum is imposed at the land boundary, assuming that Lake Erie is totally enclosed by land. The integration time step in wave hindcasting is 30 min. Also, the input wind data is linearly interpolated every 30 min and the wind at each of wave computation points set on the ray is bi-linearly interpolated by use of wind data at the surrounding 4 grid points.

3.2 Intercomparison of Wind and Wave Data

1) Time series of winds and waves

Figure 4 indicates an example for distribution of winds estimated over the lake, in case where the southwesterly strong winds blew over the lake with a tendency to converge in the northeastern area. Wind speed is greater over the central area of the lake than over the lake side affected by land topography. The feature is also found in the easterly wind conditions.

Figure 5 gives comparisons for the 3-hourly time series over one month of estimated wind speed at 10 m height U_{10} and wind direction θ_w, WAM-based and BRTM-based wave heights H_s, and BRTM-based wave period T_s against their measurement data at each of 3 buoys, in case where the measured wind speed data is transformed into 10 m height data by use of eq. (2). Either of the estimated wind speed and direction data at each buoy is generally in close agreement with the measured data, although the estimated wind speed data at B45132 tends to give a slightly smaller value than the measured data. The estimated wind direction data at B45005 tends to deviate somewhat counterclockwise from the measured data. As for wave height, both of the WAM-based and BRTM-based data follow the measured data well, which repeat growth and decay in response to wind variation. Also, time variation of the BRTM-based wave period agrees well with that of the measured data. In short, both WAM and BRTM properly reproduce time series of the measured wave height and BRTM yields a reasonable estimate for wave period, in case where space-time variation of winds over Lake Erie is evaluated with high accuracy.

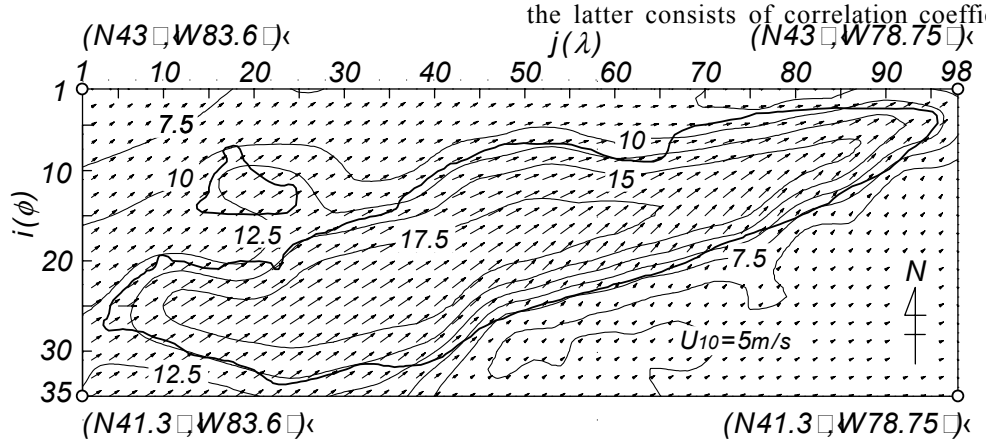

Figure 4. Example of distribution of winds estimated over Lake Erie.

2) Statistics of winds and waves, and error statistics

Figure 6 shows a scatter diagram between the estimated and measured data for 3-hourly wind speed or wind direction at each of 3 buoys. It can be said that the accuracy of the estimated wind data at each buoy is rather high, as most data are closely plotted around the perfect correlation line except for a slightly counterclockwise deviation from the measured wind direction at B45005. Table 1 summarizes wind speed statistics and error statistics of wind speed and wind direction based on the estimated and measured data. The former consists of mean value $\overline{U}_{10}$ over an entire measurement period and standard deviation U_σ for wind speed data, and the latter consists of correlation coefficient ρ_U, slope value of a regression line passing through the origin in a scatter diagram a_{0U} and root mean square error σ_U for wind speed data, and correlation coefficient ρ_θ for wind direction data. The error statistics are also given in Figure 6. Similar statistics and error statistics are calculated for wave height and wave period data. Comparison of the wind speed statistics based on the estimated and measured data and the error statistics indicate that the estimated wind data has a rather high accuracy, even though correlation coefficient for wind direction data takes apparently lower value than that for wind speed data because of its cyclic property. This suggests a possibility that the measured wind data may be assimilated into the estimated wind data.

The direction-separated occurrence rate of strong winds greater than 10 m/s is given in Figure 7, which shows that distribution of the estimated wind direction data is in close agreement with that of the measured data and that strong winds with W to SW direction were blowing over the lake during the concerned period.

Figure 8 indicates a scatter diagram between the

WAM-based or BRTM-based data and the measured data for 3-hourly wave height and correlation diagram between the WAM-based and BRTM-based wave height data at each of 3 buoys. The WAM-based wave height data yields generally a close agreement with the measured data at each of 3 buoys, but it gives a lower estimate for low wave height case and a higher estimate for high wave case at B45005 with a water depth of 14.6 m, located at the western area of the lake, and produces a lower estimate for high wave height case at B45142 with a water depth

Figure 5. Comparison of estimated or hindcast data and measured data for time series of winds and waves at each buoy(1).

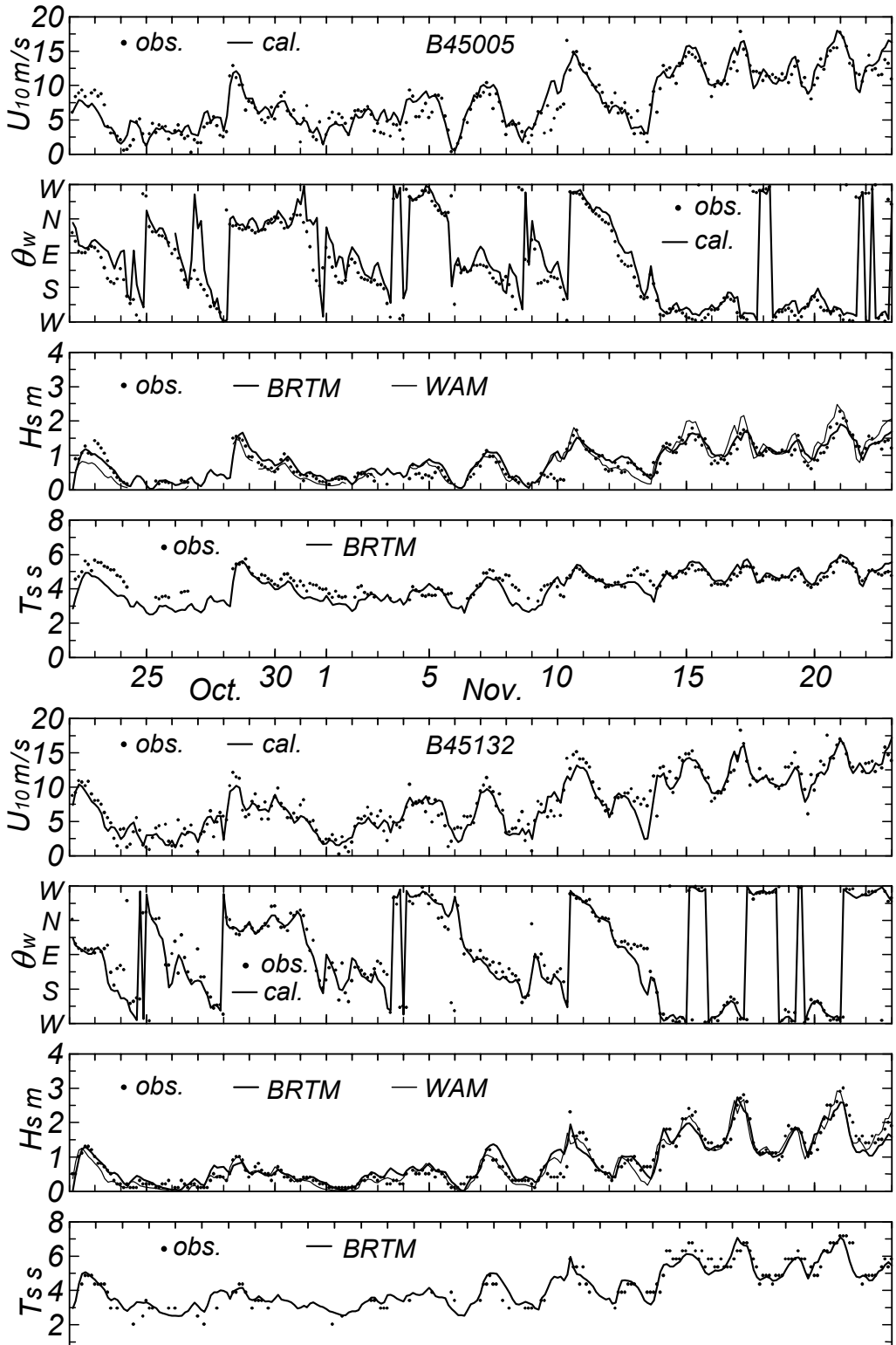

Figure 6. Scatter diagram between estimated and measure

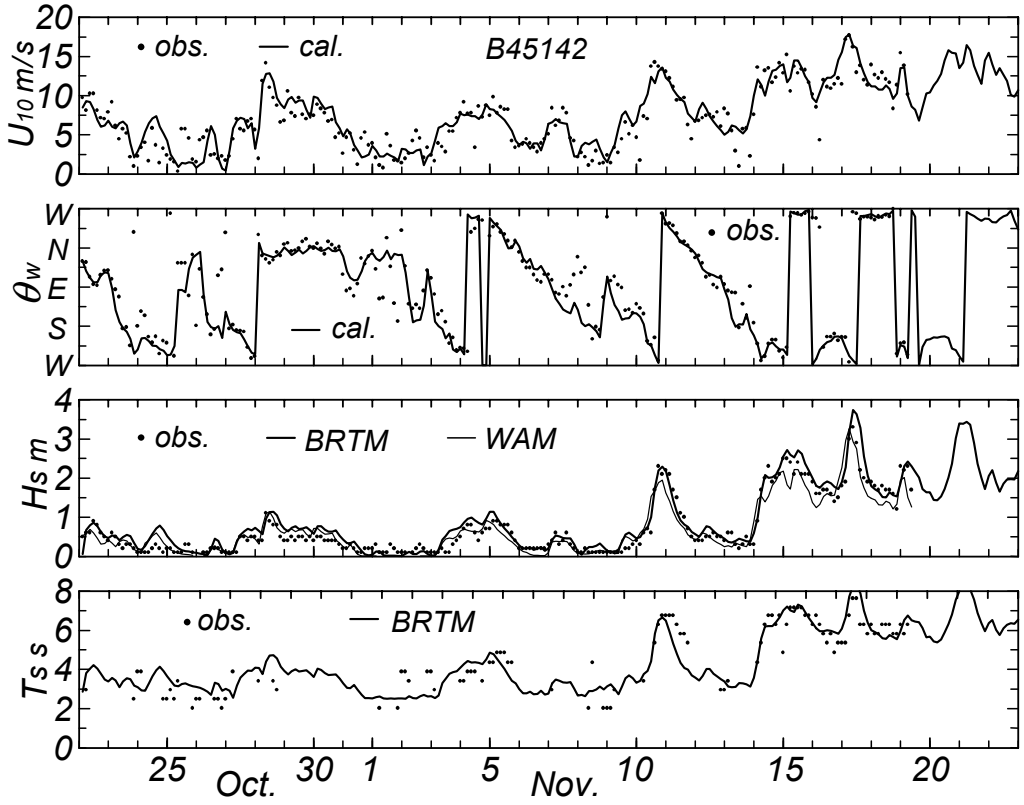

Figure 5. Comparison of estimated or hindcast data and measured data for time series of winds and waves at each buoy(2).

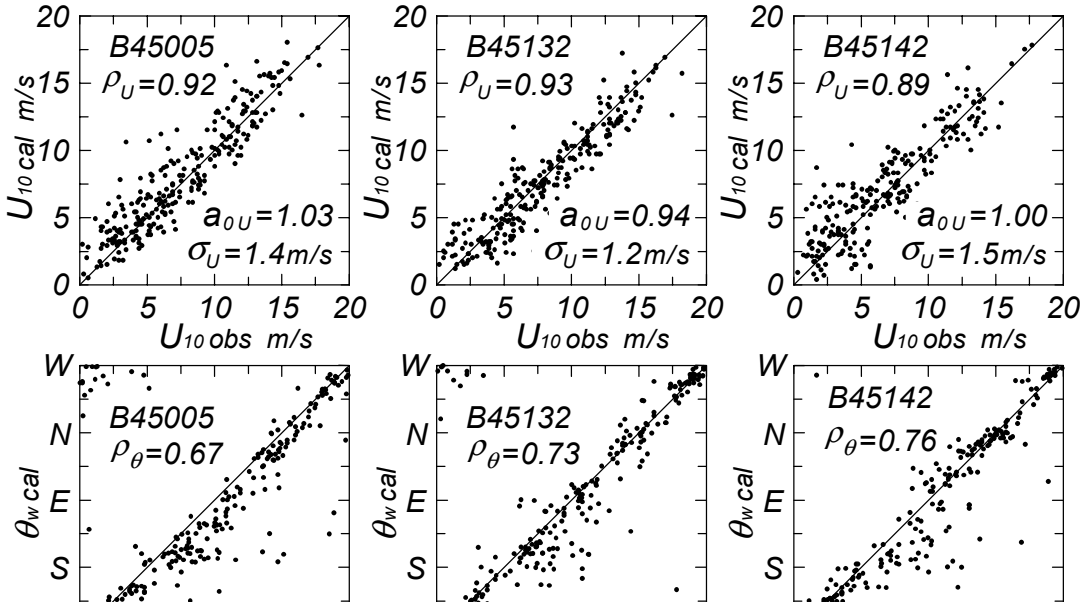

Table 1. Wind speed statistics and error statistics of wind speed and wind direction at each buoy.

buoy	$\overline{U}_{10\ \mathrm{obs}}$ m/s	$\overline{U}_{10\ \mathrm{cal}}$ m/s	$U_{\sigma\ \mathrm{obs}}$ m/s	$U_{\sigma\ \mathrm{cal}}$ m/s	ρ_U	a_{0U}	σ_U m/s	ρ_θ
45005	7.6	8.0	4.1	4.1	0.92	1.03	1.4	0.67
45132	8.0	7.7	4.1	3.9	0.93	0.94	1.2	0.73
45142	6.8	7.2	4.0	3.8	0.89	1.00	1.5	0.76

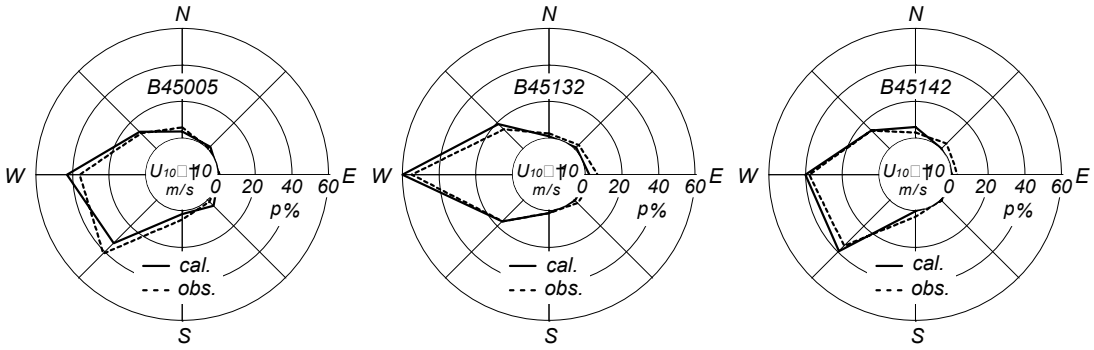

Figure 7. Comparison of direction-separated occurrence rate of strong winds at each buoy.

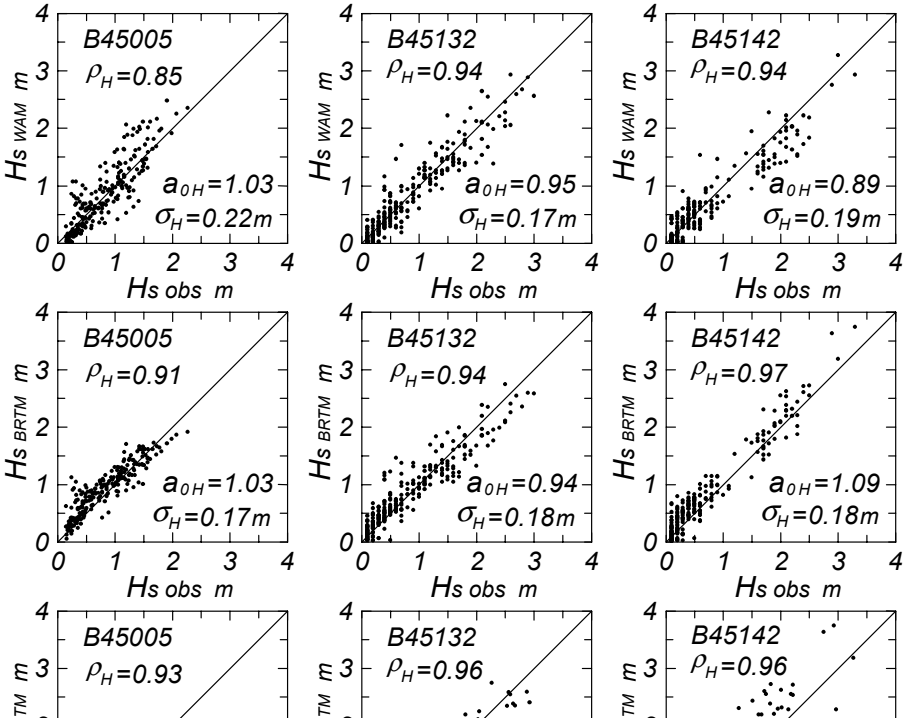

Figure 8. Scatter diagram between WAM-based or BRTM-based data a
correlation diagram between BRTM-based and WAM-based

buoy	model	$\overline{H}_{s}$ obs m	$\overline{H}_{s}$ cal m	H_{σ} obs m	H_{σ} cal m	ρ_H	a_{0H}	σ_H m
45005	WAM	0.84	**0.87**	0.48	0.58	0.85	**1.03**	0.22
	BRTM	0.84	0.93	0.48	**0.42**	**0.91**	**1.03**	**0.17**
	B-W					0.93	0.95	0.21
45132	WAM	0.85	0.82	0.69	**0.68**	**0.94**	**0.95**	**0.17**
	BRTM	0.85	**0.87**	0.69	0.61	**0.94**	0.94	0.18
	B-W					0.96	0.97	0.16
45142	WAM	0.72	**0.67**	0.74	0.67	0.94	0.89	0.19
	BRTM	0.72	0.83	0.74	**0.78**	**0.97**	**1.09**	**0.18**
	B-W					0.96	1.18	0.21

Table 2. Wave height statistics data at each buoy.

of 27 m, located at the eastern area. As well, the BRTM-based wave height data is in close agreement with the measured data to the degree comparable to the WAM-based data or to a slightly better degree, although it provides somewhat higher estimate at either B45005 or B45142 and a little lo0wer estimate for a high wave height case at B45132.

These features are found in a correlation diagram between the BRTM-based data and the WAM-based data. That is to say, the BRTM-based data is in overall agreement with the WAM-based data, except that the BRTM-based data takes a greater value for a lower wave height case and a smaller value for a large wave height case at either B45005 or B45132 and that it tends to give a little greater value on the whole at B45142.

Table 2 lists wave height statistics and error statistics obtained from the WAM-based, BRTM-based and measured data, in which the index indicating a better estimate between the WAM-based data and the BRTM-based data is printed in bold-faced type. The third line in each column describes correlation coefficient between the BRTM-based data and the WAM-based data, slope value of an origin-oriented regression line and root mean square difference. The WAM-based data gives a value closer to the measured data for mean wave height $\overline{H}_s$, but produces a significant difference for standard deviation of wave height H_σ at buoys excluding B45132. As for the error statistics at 3 buoys, correlation coefficient ρ_H ranges from 0.85 to 0.94, slope value a_{0H} from 0.89 to 1.03 and root mean square error σ_H from 0.17 to 0.22m. These values suggest that accuracy of the WAM-based data is generally rather high. On the other hand, the BRTM-based data yields a greater value than the measured data for mean wave height $\overline{H}_s$ at each of 3 buoys, but gives a value closer to the measured data for standard deviation H_σ. As for the error statistics, ranges of correlation coefficient ρ_H, slope value a_{0H} and root mean square error σ_H are from 0.91 to 0.97, from 0.94 to 1.09 and from 0.17 to 0.18 m. These values indicate that the BRTM-based data is highly correlated with the measured data, although it yields a greater estimate at B45142. In addition, the statistics such as correlation coefficient between the BRTM-based data and the WAM-based data, slope value and root mean square difference, show their high similarity. As a summary, it may be said that the BRTM-based data as well as the WAM-based data yields reasonable agreement with the measured data and that error statistics themselves may suggest a slightly higher accuracy of the BRTM-based data over the WAM-based data, although the WAM-based data gives a value closer to the measured data than the BRTM-based data for mean wave height $\overline{H}_s$.

Figure 9 demonstrates a comparison between the BRTM-based data and the measured data for 3-hourly wave period, and Table 3 summarizes the wave period statistics and error statistics. The data is plotted in a wider range around the perfect correlation line compared to wave height data case.

In spite of the result, it may be said that the BRTM-based data is in acceptable agreement with the measured data on a mean sense, as it is indicated by the wave period statistics and error statistics at each buoy.

Figure 10 compares a relation between dimensionless wave height data $\widetilde{H}_s$ and wave period data $\widetilde{T}_s$ with Toba's 3/2 power law, in which 3-hourly estimated wind speed data and BRTM-based wave height and wave period data are used. The relation is approximated by Toba's law on the whole, excluding swell-like wave data at a decaying stage. The coefficient *a*, in case where eq. (3) is fitted to a group of the data by use of the least square method is 0.056 at B45005, 0.058 at B45132 and 0.055 at B45142 respectively. These values are in close agreement with those obtained from an analysis using the measured data, and are in a range of 89 to 94 % compared to 0.062 in Toba's law. Additionally, the reason why the data with large values of dimensionless wave height and wave period found in Figure 3, is not plotted in Figure 10, is that the minimum wind speed used in BRTM-based wave

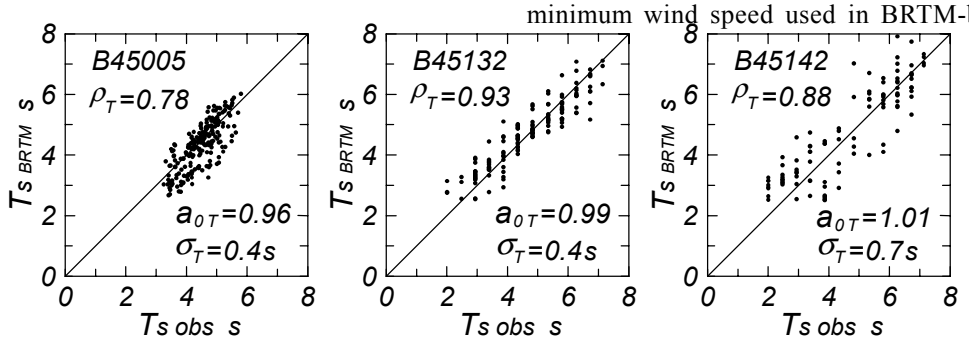

Figure 9. Comparison of BRTM-based and measured wave period data at each buoy.

Figure 10. Relation between dimensionless wave height and wave period and BRTM-based wave data.

Table 3. Wave period statistics and error statistics obtained from BRTM-based wave data and measured data.

buoy	$\overline{T}_{s}$ obs s	$\overline{T}_{s}$ cal s	T_{σ} obs s	T_{σ} cal s	ρ_T	a_{0T}	σ_T s
45005	4.5	4.3	0.6	0.8	0.78	0.96	0.4
45132	4.7	4.7	1.3	1.1	0.93	0.99	0.4
45142	4.7	4.4	1.7	1.6	0.88	1.01	0.7

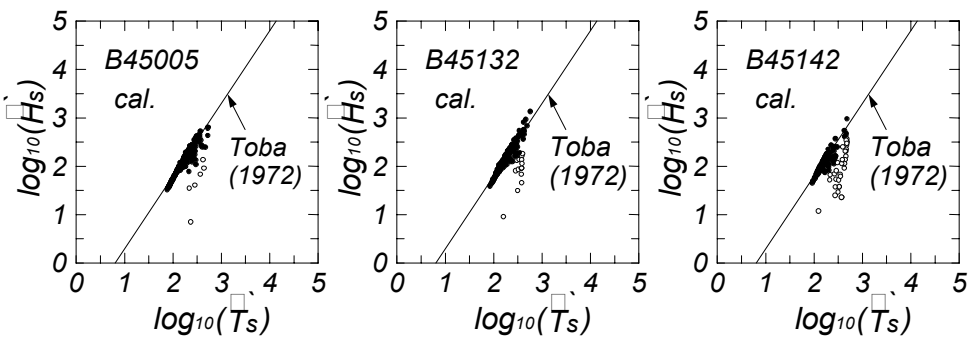

hindcasting is set to 2 m/s for the model operation.

4. CONCLUSIONS

In this study, wind and wave characteristics on Lake Erie of the Great Lakes were investigated based on the analysis of measurement data at each of 3 buoys over one month, from October 22 to November 22, 2000 and intercomparative tests were conducted using the WAM-based and BRTM-based wave data at each buoy which were calculated for the above-mentioned period under the same bathymetry and over-lake wind conditions. The obtained results are summarized as follows.

1) A relation between dimensionless wave height and wave period based on the measured data is approximated by Toba's 3/2 power law with a slightly smaller coefficient. This means predominance of wind waves during this period on the lake.
2) The wind data during this period estimated by CMC is in close agreement with the measured data at each of 3 buoys. It can be said that the CMC wind data with a high quality is most appropriate as input data to be used in wave hindcasting for testing an ability of wave prediction model.
3) As a whole, the BRTM-based wave height data yields as close an agreement with the measured data at each of 3 buoys as does the WAM-based data except for somewhat under- or over-prediction. Also, the BRTM-based wave period data agrees well with the measured data on average. As a result, a relation between dimensionless wave height and wave period obtained from the estimated wind speed data and the BRTM-based wave data is approximately satisfied with Toba's 3/2 power law, in case where the coefficient takes a slightly smaller value as well as that in a measurement-based relation.
4) Error statistics of wave height may suggest a slightly higher accuracy of the BRTM-based data over the WAM-based data, although the WAM-based data yields an estimate closer to the measured data than the BRTM-based data for wave statistics such as mean wave height.

5. ACKNOWLEDGEMENTS

The authors are very grateful to Roop Lalbeharry of the Meteorological Service of Canada, Environment Canada, who kindly provided the bottom bathymetry data, over-lake wind data estimated by CMC and WAM-based wave height data at 3 buoys.

6. REFERENCES

Booij, N., Ris, R. and L.H. Holthuijsen, 1999: A third-generation wave model for coastal regions, Part 1, Model description and validation. Jour. Geophys. Res., 104, C4, 7649-7666.

Günther, H., Hasselmann, S. and P.A.E.M. Janssen, 1992: The WAM model cycle 4(revised version). Deutsches Klima Rechen Zentrum, Technical Report, 4, 1-101.

Lalbeharry, R., Luo, W. and L. Wilson, 2001: A shallow water intercomparison on wave models on Lake Erie. Proc. WAVES2001, 1, 550-559.

Mitsuyasu, H. and T. Kusaba, 1984: Drag coefficient over water surface under the action of strong wind. Jour. Natural Disas. Sci., 6-2, 43-50.

The WAMDI Group, 1988: The WAM model- A third generation ocean wave prediction model. Jour. Phys. Oceanogr., 18, 1775-1809.

Toba, Y., 1972: Local balance in the air-sea boundary

processes 1. On the growth process of wind waves. Jour. Oceanogr. Soc. Japan, 28, 109-121.
Yamaguchi, M., Hatada, Y., Hosono, K. and M. Hino, 1984: A shallow water wave prediction model based on the radiative transfer equation. Proc. 31st Japanese Conf. on Coastal Eng., 123-127(in Japanese).
Yamaguchi, M., Hatada, Y. and Y. Utsunomiya, 1987: A shallow water wave prediction model at a single location and its applicability. Jour. Japan Soc. for Civil Engineers, 381/II-7, 151-160(in Japanese).